Impact of Temperature on the Phase Transition TiO_2 Nanoparticles

Nagaraj G (thomsun1977@gmail.com)
Periyar University PG Extension Center

Research Article

Keywords: Pure TiO2, PIM, Stability, HRTEM and UV-vis analysis

Posted Date: July 7th, 2021

DOI: https://doi.org/10.21203/rs.3.rs-273643/v2

Abstract

Unadulterated TiO2 nanoparticles have been set up by a novel Photon Induced Method (PIM) without antecedent alteration. The pre-arranged example has been calcinated at 500°C, 700°C and 1000°C to consider the impact of calcinations temperature on the security, stage and morphology of TiO2. XRD investigation uncovers an intriguing aftereffect of increment with regards to stage dependability. This might be accounted to the oxygen extravagance of the example which has been affirmed through EDAX. XRD results likewise revel a stage change from anatase to rutile with expanding calcination temperature. The morphologic examination performed with HRSEM and HRTEM revel a change from nanoparticles to nanorods. The development of TiO2 is affirmed through the Ti-O vibrational tops in FTIR and the band hole of the examples have been inspected with UV-vis Spectrophotometer. The pre-arranged examples with such high stage steadiness might be applied for photocatalytic application.

Introduction

Titania has been generally concentrated to address ecological and energy emergencies. The improvement of exceptionally dynamic heterogeneous photocatalysts has drawn in a lot of consideration lately [1-4]. Titanium dioxide has been getting impressive consideration on account of its solid oxidizing power, suitable valence band and conduction band positions, non-harmfulness and long haul dependability. In normal history, Titania has polymorphs to be specific, anatase, rutile and brookite. Anatase is a metastable stage while the rutile is a steady stage. By and large, anatase shows a lot higher photocatalytic exercises than rutile stage [5-7]. In any case, the point by point morphologies and molecule size influencing the photocatalytic action among anatase and rutile is as yet under contend. For the most part, the photocatalytic movement of Titania is strappingly reliant upon its particular surface regions, stage, design, morphologies and crystallite size [8-10]. The anatase might be accounted to its higher photocatalytic movement in light of higher surface adsorption ability to hydroxyl gatherings and a lower charge transporter recombination rate than rutile. The lower photocatalytic movement of rutile is likewise identified with its bigger grain size, lower explicit surface regions and having a more unfortunate surface adsorption limit [11-14].

Furthermore, the morphologies and glasslike size affect the exchange, detachment and portability of photogenerated electron and opening sets. In any case, the maximum capacity utilization of anatase TiO2 is hampered by its initiation just to UV light. Consequently, flow research has looked to work on the properties of Titania by stretching out the ingestion of titania to noticeable light locale [15-22]. Antecedent alteration utilizing H2O2 has been shown to be one of the successful courses to accomplish something very similar. In the current work, we propose a facial Photon Induced Method (PIM) for the readiness of oxygen-rich unadulterated anatase titania nanoparticles. Besides, clarification in regards to the fitting of the properties of the pre-arranged anatase titania, in order to use noticeable light has additionally been introduced here.

Catalyst preparation

Oxygen-rich Titania were developed by photon actuated strategy by blending required measure of Ti(OPr)4 in with 1000 ml of Double Distilled water and the arrangement is mixed for 7 hrs under the illumination of 250 W incandescent lamp. The arrangement was then left undisturbed in obscurity for 17 hrs. A similar technique is followed for 2 days. 400 ml of water is added regular day. The arrangement is kept in open spot day and night for 6 days. At long last smelling salts is added and the arrangement was presented to incandescent lamp without adding water. The last powder subsequently acquired is gathered and calcinated for 1 hr at 500°C, 700°C and 1000°C.

Results And Discussion

1.1 Powder XRD analysis

The XRD examples of the TiO2 tests calcinated at 500°C and 700°C displayed in fig. 1(a and b) are ordinarily of anatase stage TiO2 coordinating with the JCPDS No# 21-1272. No diffraction tops because of the rutile stage are noticed. This demonstrates that the incorporated examples are really of unadulterated anatase stage. The XRD example of the example calcinated at 1000°C in fig. 1c compares to average rutile stage TiO2 coordinating with JCPDS No# 21-1276. No diffraction tops due to the anatase stage are noticed. This demonstrates that the incorporated examples are really in unadulterated rutile stage when calcinated at 1000°C. It is construed that the example calcinated at 1000°C with rutile stage is exceptionally glasslike; this is affirmed by the low worth of its Full Width Half Maximum (FWHM). This is likewise demonstrative of a huge crystallite size of 110 nm for test calcinated at 1000°C while the crystallite size of 10 nm and 15 nm is gotten for tests calcinated at 500°C and 700°C separately.

HRSEM and HRTEM Micrograph analysis

Fig. 2 (an and b) shows the HRSEM micrographs to consider the surface morphology of anatase and rutile tests. Anyway no unmistakable data could be accumulated aside from the presence of ungainly particles. The HRTEM picture clearly shows the morphology as circular nanoparticles of size 32 nm and 45 nm as found in fig. 3(a and b), comparing to tests calcinated at 500°C and 700°C separately. While the micrograph in fig.3c relating to the TiO2 test calcinated at 1000°C, shows nanopartricles and nanorod like morphologies. The estimation of the disconnected nanorod is 210 nm wide and 350 nm length (fig.3c). This outcomes affirm the increment in molecule size as the calcination temperature is expanded. Also a transformatiom of morphology from nanoparticles to nanorod is seen alongside the stage change from anatase to rutile.

FTIR analysis

Fig. 4 shows the FTIR spectra of tests calcinated at 500°C, 700°C and 1000°C with anatase and rutile stages. The top around 1043 cm−1 might be because of C-O extending [23]. The top around 1656 cm−1 relate to the hydroxyl gatherings of sub-atomic water [24] and an expansive top at 3430 cm−1 for the O-H extending vibrations. The little tops at 2854 and 2921 cm−1 in the range might be credited to the CH2 extending vibrations [25]. Fig.4 (an and b) shows the FTIR estimation for the anatase stage TiO2

calcinated at 500°C and 700°C examples. It tends to be seen that the forces of retention groups of oxygen-containing utilitarian gatherings like C-O (1043 cm−1) are step by step diminished with expansion in calcinations temperature. This outcomes demonstrate that as the calcination temperature is expanded, the oxygen content in the example is decreased. The range additionally showed solid retention groups at 720 cm−1 demonstrating the presence of Ti-O-Ti bond in TiO2 as displayed in fig 4(a, b and c) [26].

UV-vis analysis

UV-noticeable (UV−vis) spectroscopy has been demonstrated to be a compelling optical characterizationtechnique to comprehend the bandgap of semiconductors. The optical band hole of TiO2 are resolved utilizing a Tauc plot as displayed in Fig. 5(a, b and c). The surmised band hole of unadulterated TiO2 test calcinated at 500°C, 700°C and 1000°C are 3.2 eV, 3.08 eV and 2.97 eV separately. This upheld the subjective perception of a red change in the assimilation edge of the unadulterated anatase stage TiO2 calcinated at 700°C contrasted with the example calcinated at 500°C. The narrowing of band hole could be attributed to the synthetic holding (oxygen-rich) among TiO2 and the particular destinations of carbon during the Photon prompted strategy.

Conclusion

The photon initiated technique is utilized to plan oxygen rich TiO2. The constructions, morphology and band hole of the example has been examined concerning expansion in calcinations temperature. XRD result show that, as the calcinations temperature builds an anatase to rutile stage change is seen. In addition, the increment in top powers recommends a diminishing in full width at half most extreme which thusly uncovered an expansion in crystallite size. The HRTEM pictures show a morphology change from nanoparticles to nanorods with expanding calcinations temperature. This proposes that calcinations temperature additionally assumes an imperative part in coordinating the morphology and glasslike nature. The optical bandgap determined shows a diminishing pattern with expansion in calcination temperature. In this way the band hole of the oxygen-rich TiO2 arranged by PIM is designed in order to assimilate energy in the apparent light district. This will open new knowledge into different applications, for example, photocatalytic action, sun oriented cells, antibacterial action, killing of malignant growth cells, etc.

Experimental Part

Materials. Catharanthus Roseus plants were provided from Dharmapuri District. The plants were cleaned with H_2O to eliminate dust and unwanted materials and it was grinned with filtered.

Nano-size plant powder preparation. The green synthesis of the plant under the photo-induced method was used for the solvent extraction procedure. About 200 ml of plant dispersion was added in 1000 ml of deionized water for 25 days under light irradiation. The resulted product was dried and annealed at 110 °C for 60 min. Characterizations Techniques: XRD patterns of the samples were monitored on a Bruker D8

Advance powder X-ray diffractometer with Cu-Kα (λ = 1.5406 Å). Elemental compositions were measured by EDX analysis (Hitachi S-4800). The morphology of NPs was ascertained via TEM (JEM-2100F). Fourier transforms infrared (FTIR) spectra of the NPs were recorded using the KBr pellet technique (Bruker, Tensor 27 spectrometer). Particle size and Z-average of samples were characterized using DLS analysis (Horiba). UV-vis Diffuse reflectance spectroscopy (UV-DRS) was obtained with a Perkin Elmer Lambda 25 spectrometer.

GC/MS analysis. GC/MS (Clarus 680 GC) was used to elucidate the existence of active constituents and the chemical composition of CR-NPs. GC/MS was accomplished employing a fused silica column consists of Elite-5MS with 95% dimethylpolysiloxane, 5% biphenyl, and 30 m × 0.25 mm ID × 250μm df. The Helium was used as carrier gas to separate the components with 1 ml/min flow. The operation temperature was maintained at 260 °C during the chromatographic process. The plant material (1μL) was applied into the device and the temperature rate was set at: 60 °C (120 s); 300 °C at the rate of 10 °C min^{-1}; and 300 °C. The mass detector was operated at: 230 °C transfer line temperature; 230 °C ion source temperature; and ionization mode electron impact at 70 eV, a scan time of 0.2 s and scan interval of 0.1 s. The spectrum of the component was compared with the data of the of known component kept in the GC-MS NIST (2008) library.

In vitro cytotoxicity of the CR-NPs Procedure. The MCF 7 cancerous and VERO normal cells were provided from National Centre for Cells Sciences. The cells were supplemented 10% fetal bovine serum (FBS) in Eagle's MEM. The samples were attained at 37ºC with 5% carbon dioxide and 95% air conditions. The culture medium was checked and maintained frequently as well as replaced twice a week.

Cells treatment protocol. The cultured cells were separated with trypsin ethylene diamine tetra acetic-acid, then viable cells were measured employing a diluted hemo-cytometer possess 5% FBS ($1x10^5$ cells/ml). Afterward, a 0.1 ml of cells solutions were added into 96-well plate at a density of 10,000 cells/well. The cells were incubated at 37 ºC with 5% carbon dioxide and 95% air. After one day of incubation, the suspensions were modified with serial contents of the prepared NPs. The samples were dispersed in dimethylsulfoxide and sample dispersion was diluted twice and the required final test amount with serum free medium. Another four serial dilutions were performed to provide a total of five sample concentrations. A solutions of 0.1 ml of the diluted samples were inserted to the suitable wells, which having 0.1 ml of cultured media. The plates were maintained for two days at 37 ºC with similar conditions. The medium-only sample was acted as reference and triplicate was attained for all contents.

MTT assay. The mitochondrial enzymes in organ cell called succinatedehydrogenase cleave the tetrazolium and dissolving the MTT to an insoluble purple formazan. Thus, the produced formazan is precisely proportional to the viable cells number. After 2 days, 15 µl of MTT (5 mg/ml) in phosphate buffered saline was seeded to each well and kept at 37 ºC for 4 h. Then, the media with MTT were flicked off and the developed formazans were added in 100 µl of DMSO. Finally, the absorbance was recorded at 570 nm utilizing micro-plate reader.[28, 29]

Declarations

NOTES

The authors declare no competing financial interest.

ACKNOWLEDGMENTS

The authors thank director Dr. P. Mohana Sundram PG Extension Center, Periyar University, Tamilnadu, India

References

1. Machida, W.K. Norimoto, T. Kimura. Antibacterial Activity of Photocatalytic Titanium Dioxide Thin Films with Photodeposited Silver on the Surface of Sanitary Ware. *J. Am. Ceram*. Soc. 88, 95-100, 2005
2. M. Hermann, J. Pichat Disdier. Effect of chromium doping on the electrical and catalytic properties of powder titania under UV and visible illumination *P. Chem. Phys. Lett.* 108, 618-622, 1984
3. R. Ayers, A.J.Hunt. Titanium oxide aerogels prepared from titanium metal and hydrogen peroxide. *Mater. Lett. 34*, 290, 1998
4. F. Zhang, Y.L. He, M.S. Zhang, Z. Yin, Raman scattering study on anatase TiO_2 nanocrystals. *J. Phys. D: Appl. Phys*. *33*, 912–916, 2000
5. Lin, A. Orlov, R.M. Lambert, M.C. Payne. New Insights into the Origin of Visible Light Photocatalytic Activity of Nitrogen-Doped and Oxygen-Deficient Anatase TiO_2. *J. Phys. Chem. B*. *109*, 20948-20952, 2005
6. Inagaki, R. Nonaka, B. Tryba, A.W. Morawski. Dependence of photocatalytic activity of anatase powders on their crystallinity. *Chemosphere. 64*, 437-445, 2006
7. Fujishima, X. Zhang, D.A. Tryk. TiO_2 photocatalysis and related surface phenomena Surf. Sci. Rep. 63, 515-582, 2008
8. L. Linsebigler, G. Lu, J.T. Yates. Photocatalysis on TiOn Surfaces: Principles, Mechanisms, and Selected Results. *Chem. Rev. 95*, 735-758, 1995
9. Branek, H. Kisch. Tuning the optical and photoelectrochemical properties of surface- modified TiO_2. *Photochem. Photobiol. Sci. 7*, 40-43, 2008
10. D. Shannon, Phase Transformation Studies in TiO_2 Supporting Different Defect Mechanisms in Vacuum-Reduced and Hydrogen-Reduced Rutile. *J. Appl. Phy. 35*, 3414-3416, 1964
11. R. Torres, T. Lindgren, J. Lu, C.-G. Granqvist, S.-E. Lindquist. Highly visible light active TiO_2–x Nx Heterojunction Photocatalysts. *Phys. Chem. B*. *108*, 5995- 6003, 2004
12. Lida, S. Ozaki. Grain Growth and Phase Transformation of Titanium Oxide during Calcination. *J. Am. Ceram. Soc. 44*, 120-127, 1961

13. Ohsaka, S. Yamaoka, O. Shimomura. Effect of hydrostatic pressure on the Raman spectrum of anatase (TiO_2). *Solid State Commun. 30*, 345–347, 1979
14. A. Gao, A.P. Xian, L.H. CaO, R.C. Xie. Influence of calcining temperature on photoresponse of TiO_2 film under nitrogen and oxygen in room temperature. Sens. *Actuators B Chem. 134*, 718-726, 2008
15. L-L. Tan, -J. Ong, S.-P. Chai, A.R. Mohamed. Reduced graphene oxide- TiO_2 nanocomposite as a promising visible-light-active photocatalyst for the conversion of carbon dioxide.*Nanoscale Res. Lett. 8,* 465-468, 2013
16. Etacheri, M.K. Seery, S. J. Hinder, S. C. Pillai, Oxygen Rich Titania: A Dopant Free, High Temperature Stable, and Visible-Light Active Anatase Photocatalyst. *Adv. Funct. Mater. 21*, 3744-3752, 2011
17. H. Hanaor, C. Sorrell, Review of the anatase to rutile phase transformation. *J.Mater.Sci. 46*, 855-874, 2011
18. Pei, J. Luan, Development of visible light-responsive sensitized photocatalysts. *Int. J. Photoenergy***.** 13, 2012
19. -L. Tan, W.-J. Ong, S.-P. Chai, A.R. Mohamed. Band gap engineered, oxygen-rich TiO_2 for visible light induced photocatalytic reduction of CO_2.*Chem. Commun.* 50, 6923–6926, 2014
20. Nagaraj, A. Dhayal Raj, A. Albert Irudayaraj, Next Generation of Pure Titania Nanoparticles for Enhanced Solar- Light Photocatalytic Activity. Materials science: Materials in Electronics. 1-9, 2017
21. Zang. Visible-light detoxification and charge generation by transition metalChloride modified titania. *Chem. Euro. J. 6*, 379–384, 2000
22. Zhou, Y. Zhu, X. Yang, X. Jiang, C. Li. Preparation of graphene-TiO_2 composites with enhanced photocatalytic activity. New J Chem. 35(2):353–359, 2011
23. Pan, J.J. Zou, S. Wang, X.Y. Liu, X. Zhang, L. Wang. Morphology evolution of TiO_2 facets and vital influences on photocatalytic activity. ACS Appl Mater Interfaces. 4(3), 1650–1655, 2012
24. S.Sher Shah, A.R.Park, K. Zhang, J.H. Park, P.J. Yoo. Green synthesis of biphasic TiO_2-reduced graphene oxide nanocomposites with highly enhanced photocatalytic activity. ACS Appl Mater Interfaces. 4(8):3893–3901, 2012
25. Yang, J. Zhai, D. Wang, Y. Chen, L. Jiang. Two-dimensional grapheme bridges enhanced photoinduced charge transport in dye- sensitized solar cells. ACS Nano 4(2):887–894, 2010

Figures

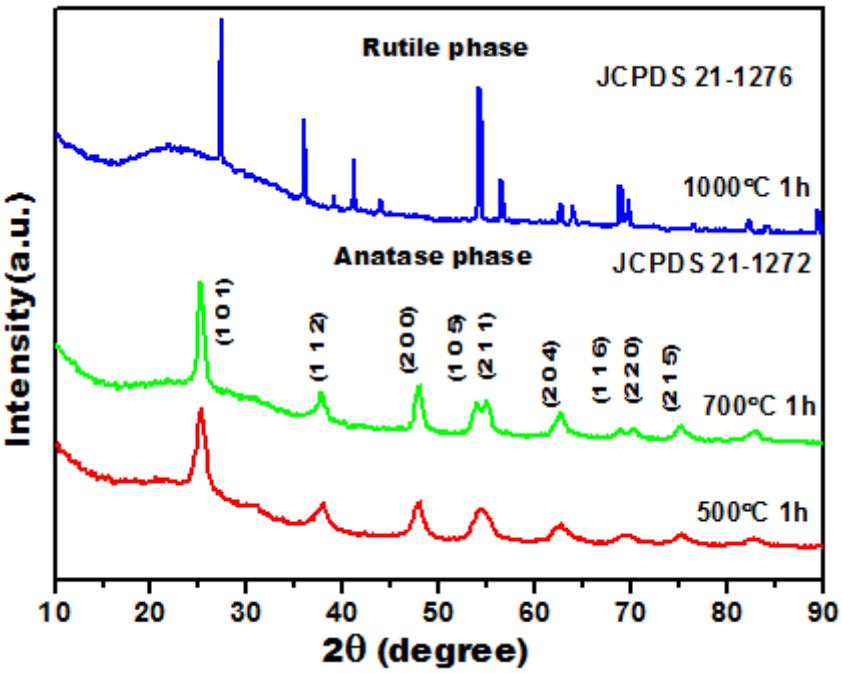

Figure 1

The power XRD patterns of TiO2 sample calcinated at (a) 500°C, (b) 700°C and (c)1000°C

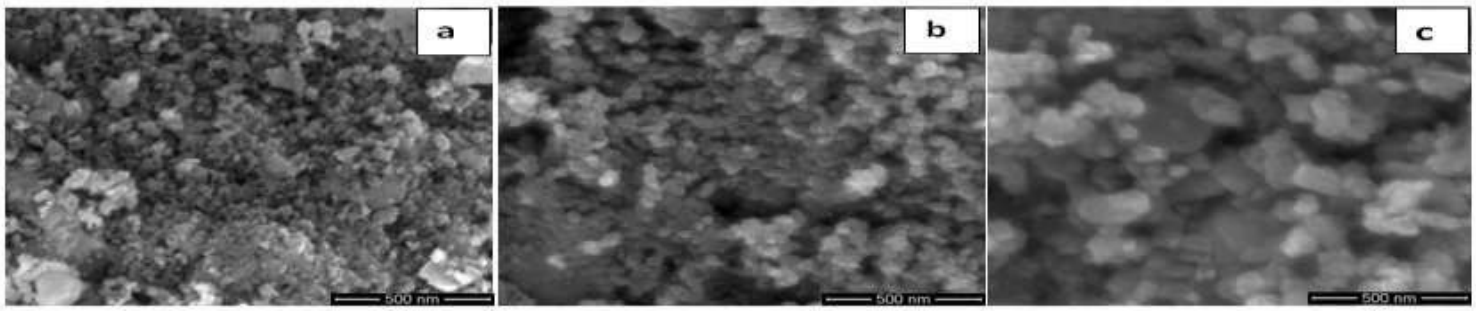

Figure 2

HRSEM images of TiO2 sample calcinated at (a) 500°C, (b)700°C and (c)1000°C

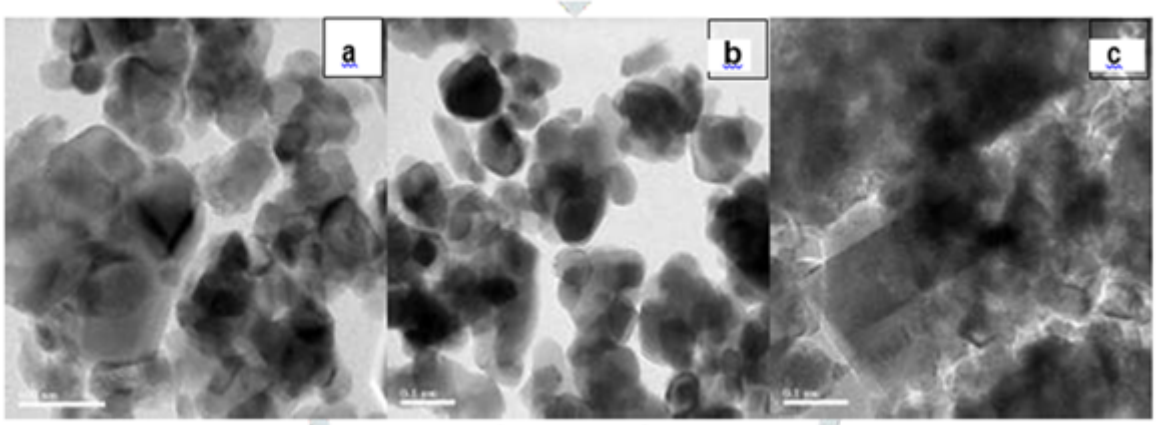

Figure 3

HRTEM images of TiO2 sample calcinated at (a) 500°C, (b) 700°C and (c)1000°C

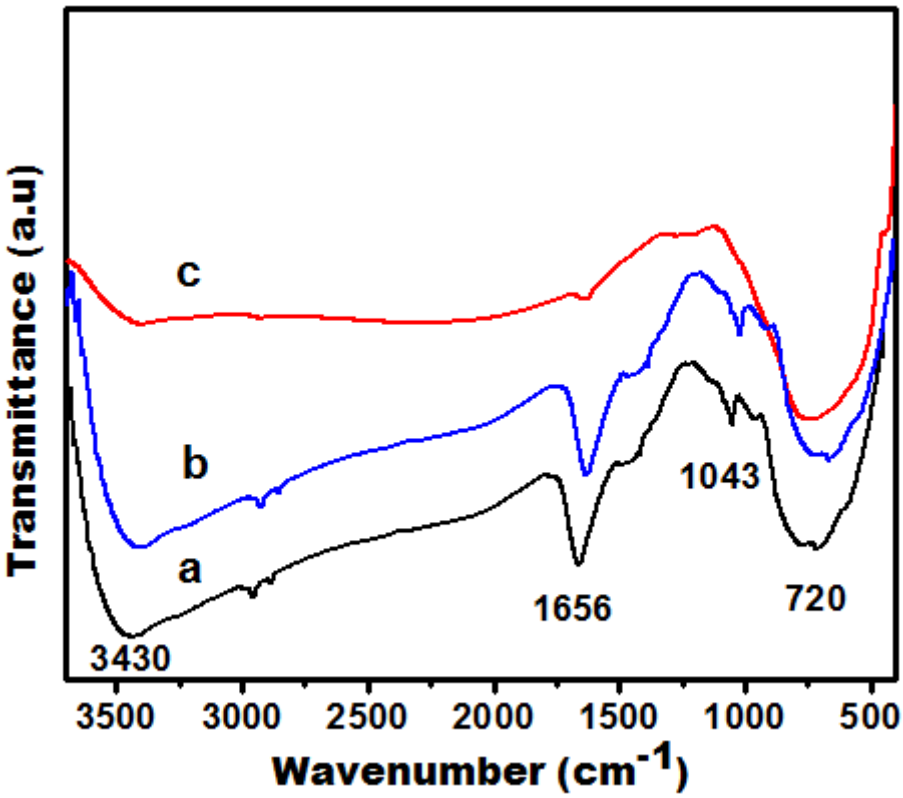

Figure 4

FTIR spectrum of TiO2 sample calcinated at (a) 500°C, (b)700°C and (c)1000°C

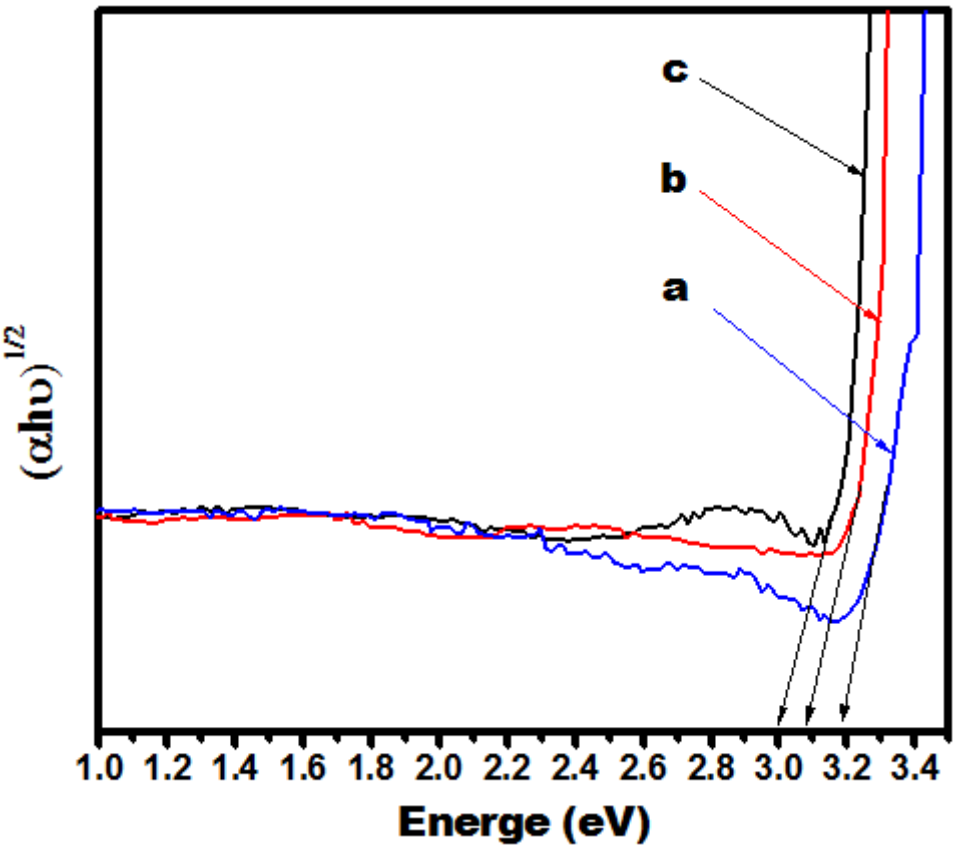

Figure 5

UV-visible spectroscopy of TiO2 calcinated at (a) 500°C, (b)700°C and (c)1000°C